

Assessment of Afforestation and Deforestation and Tree Cover with NDVI and LST Using Sentinel-2 and Landsat 8 Imagery Through Google Earth Engine in the Tawi Watershed, Jammu District, Jammu and Kashmir, India

Meenu Sharma¹; Rakesh Verma^{2*}; Sundeep Pandita³; Rajwant⁴; Ahsan Ul Haq³

¹Department of Geology, Cluster University of Jammu, Jammu 180001, India.

²Jammu and Forest Services, India

³Department of Geology, University of Jammu 180006, India.

⁴Anusandhan National Research Foundation, New Delhi 110016, India

Corresponding Author: Rakesh Verma^{2*}

Publication Date: 2026/02/28

Abstract: This study evaluates vegetation cover changes in the Tawi watershed of Jammu District between 2019 and 2024 using Landsat 8 and Sentinel-2 satellite imagery and machine learning techniques. Central to the analysis is the calculation of the Normalized Difference Vegetation Index (NDVI), Land Surface Temperature (LST) and the estimation of tree cover to detect spatial and temporal vegetation dynamics. Data processing and analysis were conducted through Google Earth Engine (GEE), employing a machine learning-based classification workflow to enhance accuracy and monitoring efficiency. The methodology encompasses data acquisition, pre- and post-classification comparisons, identification of key challenges, and interpretation of findings. The integrated analysis suggests a strong inverse relationship between NDVI and LST values in which areas with lower vegetation cover (low NDVI) correspond to higher surface temperatures (high LST) particularly in April 2024. The linear correlation between NDVI and LST usually reflect “Weak negative”, “Moderate negative” and “Very weak negative” in the Tawi watershed. This trend reflects potential land cover changes such as vegetation loss, urban expansion, or soil exposure, contributing to higher heat absorption and reduced evapo-transpiration. The results reveal significant vegetation changes over the five-year period: No Vegetation (Unchanged) – 32%, Afforestation – 5%, Deforestation – 12%, and Vegetation (Unchanged) – 51%. These findings underscore the value of integrating remote sensing and machine learning for ecological monitoring. The study concludes with strategic recommendations for sustainable landscape management and advocates for resilient, technology-driven frameworks in future environmental assessments.

Keywords: NDVI; Tree Cover; Tawi Watershed; Sentinel 2; Afforestation; Deforestation, LST.

How to Cite: Meenu Sharma; Rakesh Verma; Sundeep Pandita; Rajwant; Ahsan Ul Haq (2026) Assessment of Afforestation and Deforestation and Tree Cover with NDVI and LST Using Sentinel-2 and Landsat 8 Imagery Through Google Earth Engine in the Tawi Watershed, Jammu District, Jammu and Kashmir, India. *International Journal of Innovative Science and Research Technology*, 11(2), 1982-1997. <https://doi.org/10.38124/ijisrt/26feb977>

I. INTRODUCTION

The environmental system encompasses biodiversity, climatic variations, and the overall health of natural ecosystems. However, the unprecedented rate of urbanization, driven by changing demographic patterns, has significantly impacted these systems by altering atmospheric components at a regional level. One of the most critical consequences is large-scale deforestation, which leads to

habitat loss, increased greenhouse gas emissions, and disruptions in the hydrological cycle.

Natural vegetation comprising plant life that grows without direct human intervention—is particularly sensitive to global climatic variations. Changes in temperature and precipitation patterns throughout the year, as reflected in land surface temperature (LST), directly influence vegetation health and distribution. As such, effective monitoring of deforestation becomes essential. It plays a vital role in

strategic planning and the development of mitigation measures aimed at achieving sustainable land management.

Field surveys are often impractical in large, inaccessible areas due to their labor-intensive nature and high economic costs. To overcome these limitations and obtain real-world observations, satellite imagery combined with machine learning techniques offers a powerful alternative. This approach enables contextual, comprehensive, and near real-time monitoring of the Earth's surface, making it highly effective for environmental assessment and decision-making. Sentinel-2, a satellite mission under the European Space Agency's Copernicus program, provides high-resolution multispectral imagery that is particularly well-suited for vegetation analysis. It captures data across visible, near-infrared (NIR), and shortwave infrared (SWIR) spectral bands—critical for assessing vegetation health and detecting changes in forest cover. With its frequent revisit times and global coverage, Sentinel-2 enables continuous and reliable monitoring of terrestrial ecosystems, making it an invaluable tool for environmental assessment and land management.

The Normalized Difference Vegetation Index (NDVI) is one of the most widely used vegetation indices for satellite-based assessment and monitoring of global vegetation and growth productivity over the past two decades (Huete and Lui, 1994; Leprieur et al., 2000; Scanlon et al., 2002; Kunkel et al., 2011). This index has been proved to be key technique for the assessment of vegetation health which is calculated from the NIR and red bands of the spectrum using formula (Tucker, 1979):

$$NDVI = (NIR + Red) / (NIR - Red)$$

Higher NDVI values typically indicate healthy vegetation, as they correspond to greater reflection in the near-infrared (NIR) band and increased absorption of red light. Conversely, lower NDVI values are associated with deforested or sparsely vegetated areas, making NDVI an effective tool for monitoring deforestation and vegetation degradation.

Land Surface Temperature (LST) is a widely used parameter for assessing the exchange of energy between Earth's surface features and the atmosphere, plays a crucial role in understanding the variations in radiant temperature, which is essential for analyzing changes in surface temperature patterns (Anbazhagan and Paramasivan, 2016). The Normalized Difference Vegetation Index (NDVI) is a dominant factor in the derivation of Land Surface Temperature (LST) and is consistently utilized in LST-related studies (Smith and Choudhury, 1990; Julien et al., 2006; Yuan XL et al., 2017).

The present study uses Sentinel-2 imagery, Landsat 8 and NDVI to monitor deforestation, correlation of NDVI and LST to infer changes in the Tawi watershed. By processing satellite data to calculate NDVI and applying thresholding techniques, we can identify and visualize deforested areas. The methodology includes accessing satellite imagery, calculating NDVI, classifying deforested areas, and visualizing results. These steps are crucial for accurately detecting and analyzing deforestation. The insights from this project will enhance our understanding of deforestation dynamics and support conservation and policy efforts. This project also lays the groundwork for future integration of advanced machine learning methods to improve deforestation detection accuracy and automation. Effective use of satellite imagery and analytical techniques will provide timely, accurate information to aid in preserving and sustainably managing forested areas.

The primary environmental concern addressed in this paper is the vegetation pattern of the watershed. The main objectives of the present study covers.

- To create NDVI maps of the Tawi watershed
- To analyse change in land surface temperature (LST) data during 2019 and 2024
- To detect change in deforestation and afforestation pattern in the Tawi watershed

II. MATERIALS AND METHODS

➤ Study Area

The Tawi watershed covering an area of 835 sq. km. is located in the Jammu District, Union Territory of Jammu and Kashmir (Fig. 1). The Tawi River basin lies between 74°35' to 75°45' E longitudes and 32°35' to 33°05' N latitudes. Physiographically, it is divided into the Siwalik and Outer Plain areas, situated at the foothill zone of the Himalayan belt (CGWB, 2013). The geology of the catchment comprises the Murree and Siwalik Group of rocks, which include consolidated and semi-consolidated conglomerates, sandstones, shales, siltstones, and claystones. According to the classification by Karunakaran and Ranga Rao (1979), the Siwalik Group is subdivided into: Lower Siwalik: thick-bedded sandstones, mudstones, and siltstones, Middle Siwalik: medium to coarse and pebbly sandstones, Upper Siwalik: mudstones and conglomerates with occasional sand and clay lenses.

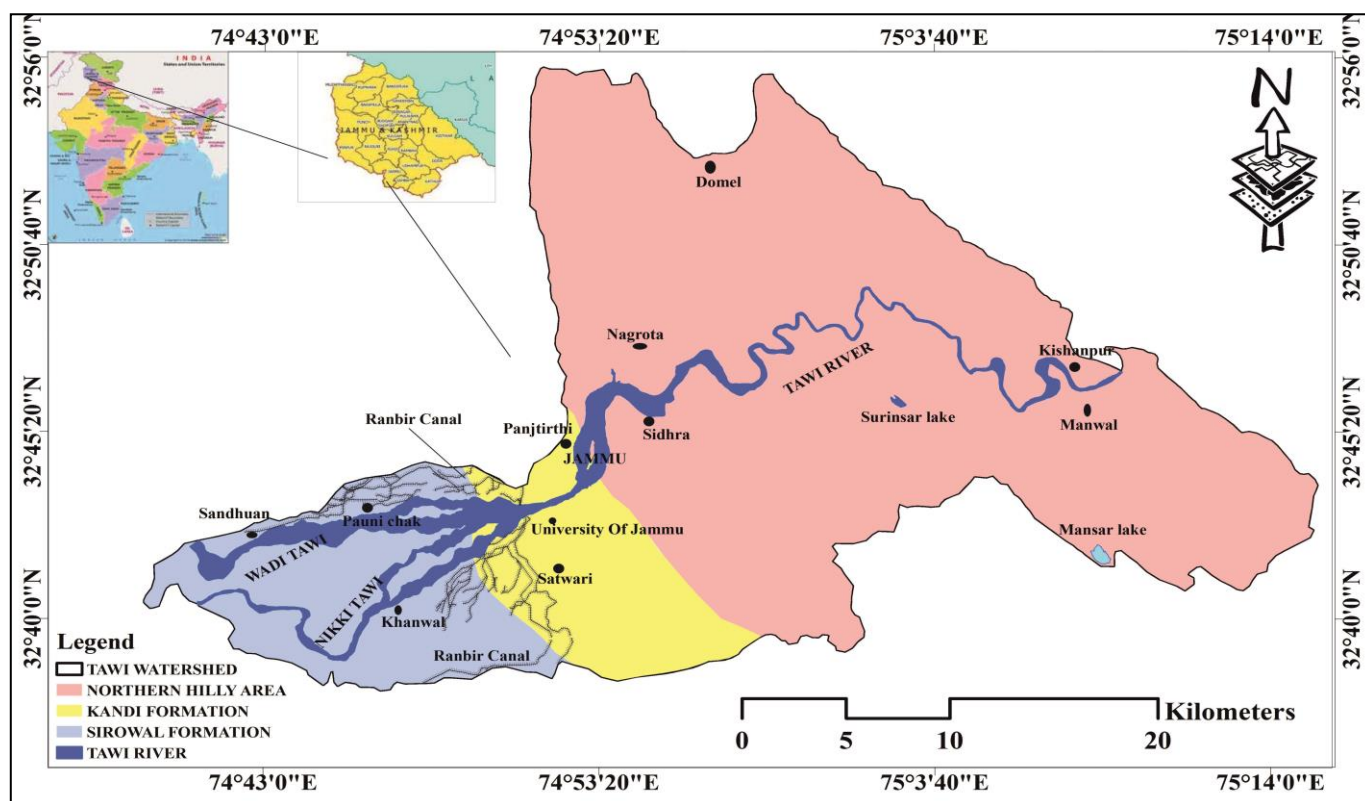


Fig 1 Location Map of the Tawi Watershed.

➤ *Geospatial Data*

• *Satellite Imageries*

For the calculation of NDVI, “Harmonized Sentinel-2 Multi Spectral Instrument (MSI), Level- 2A (SR) imagery was used while the land surface temperature (LST) was

calculated from “Landsat 8” imagery. ARCGIS 10.7.1 was used for the presentation of NDVI, LST and Afforestation-Deforestation maps.

Table 1 MSI Sentinel- 2A (SR) Imagery Datasets

| Band name (Spatial resolution) | Wavelength (nm) | Scale | Description |
|--------------------------------|-----------------|--------|-------------|
| B1- 60 m | 443.9 | 0.0001 | Aerosols |
| B2- 10 m | 496.6 | 0.0001 | Blue |
| B3- 10 m | 560 | 0.0001 | Green |
| B4- 10 m | 664.5 | 0.0001 | Red |
| B5- 20 m | 703.9 | 0.0001 | Red Edge 1 |
| B6- 20 m | 740.2 | 0.0001 | Red Edge 2 |
| B7- 20 m | 782.5 | 0.0001 | Red Edge 3 |
| B8- 10 m | 835.1 | 0.0001 | NIR |
| B8-A- 20 m | 864.8 | 0.0001 | Red Edge 4 |
| B9- 60 m | 945 | 0.0001 | Water vapor |
| B11- 20 m | 1613.7 | 0.0001 | SWIR 1 |
| B12- 20 m | 2202.4 | 0.0001 | SWIR 2 |

(Source: European Union/ESA/Copernicus)

• *Machine Learning (GEE)*

Machine learning is revolutionizing areal (spatial) analysis by reducing reliance on field surveys and manual interpretation. Under this, Google Earth Engine (GEE) is a cloud-based service providing interpretation of earth surface changes, its trends and patterns using geospatial datasets and imageries (Molnar and Kiraly., 2023). Google Earth Engine provides users with enormous access to European Union, ESA, and Copernicus datasets (e.g., Sentinel, land cover,

climate variables) directly through its web-based code editors, supporting both JavaScript (via the Code Editor) and Python (via APIs, Colab, Jupyter, and browser-embedded runtimes).

➤ *Computation of Land and Surface Temperature Using Landsat 8 in ARCGIS*

For the computation of LST, the Landsat 8 thermal band (band 10 and 11) has been employed (Ihlen and Zanter, 2019).

The five steps procedure is used for processing the Landsat-8 satellite imagery in the software ARCGIS 10.7.1.

➤ *To Calculate Top of Atmosphere (TOA) Spectral Radiance:*

The use of radiance rescaling factor is used to convert Thermal Infra-Red Digital Numbers to TOA spectral radiance.

$$L\lambda = ML * Q_{cal} + AL - O_i$$

Where:

$L\lambda$ = TOA spectral radiance (Watts/(m² * sr * μm))

ML = Radiance multiplicative Band (No.)

AL = Radiance Add Band (No.)

Q_{cal} = Quantized and calibrated standard product pixel values (DN)

O_i = correction value for band 10 is 0.29

• *To convert Top of Atmosphere (TOA) to Brightness Temperature (BT):*

The spectral radiance data can be converted from Top of Atmosphere (TOA) to Brightness Temperature (BT) using the thermal constant values in Meta data file:

$$\text{Kelvin (K) to Celsius (°C) Degrees } BT = K2 / \ln(K1 / L\lambda + 1) - 273.15$$

Where:

BT = Top of atmosphere brightness temperature (°C)

$L\lambda$ = TOA spectral radiance (Watts/m² * sr * μm)

K1 = K1 Constant Band (No.)

K2 = K2 Constant Band (No.)

• *To Calculate Normalized Difference Vegetation Index (NDVI):*

The Normalized Difference Vegetation Index (NDVI) is a standardized vegetation index which is calculated using Near Infra-Red (Band 5) and Red (Band 4) bands.

$$NDVI = (NIR - RED) / (NIR + RED)$$

$$NDVI = (\text{Band 5} - \text{Band 4}) / (\text{Band 5} + \text{Band 4})$$

Where:

RED = DN values from the RED band

NIR = DN values from the Near-Infrared band

• *To Calculate Land Surface Emissivity (LSE):*

Land surface emissivity (LSE) is the average emissivity of an element of the surface of the earth calculated from NDVI values.

$$PV = ((NDVI - NDVI_{min}) / (NDVI_{max} - NDVI_{min}))^2$$

Where:

PV = Proportion of Vegetation

NDVI = DN values from NDVI image

NDVI_{min} = Minimum DN values from NDVI image

NDVI_{max} = Maximum DN values from NDVI image

$$E = 0.004 * PV + 0.986$$

Where:

E = Land Surface Emissivity

PV = Proportion of Vegetation

• *To Calculate Land Surface Temperature (LST)*

The Land Surface Temperature (LST) is the radiative temperature which calculated using Top of atmosphere brightness temperature, wavelength of emitted radiance and Land Surface Emissivity.

$$LST = BT / (1 + (\lambda * BT / c2) * \ln(E))$$

Where:

BT = Top of atmosphere brightness temperature (°C)

λ = Wavelength of emitted radiance

E = Land Surface Emissivity

c2 = 14388 mk

III. METHODOLOGY

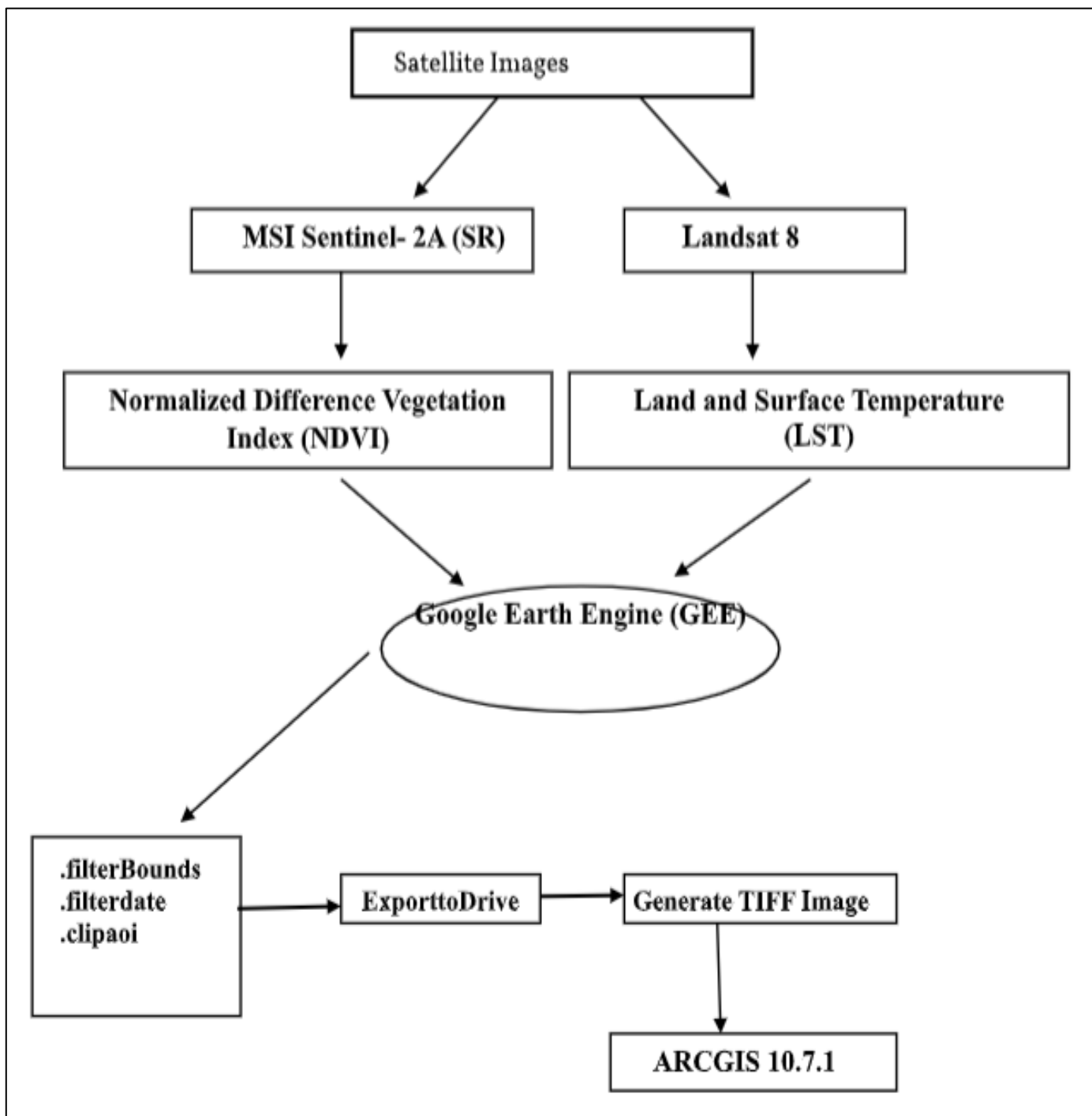


Fig 2 Flowchart Showing the Steps Used for the Evaluation of NDVI and LST

IV. RESULTS

➤ Normalized Difference Vegetation Index (NDVI)

In 2019, the NDVI values in the Tawi watershed ranged from a minimum of -0.177 to a maximum of 0.765 (Fig. 3). In 2024, the NDVI range extended from -0.39 to 0.833 (Fig. 4). Despite the wider range in 2024, the mean NDVI was slightly higher in 2019 recorded at 0.51, compared to 0.50 in 2024. The NDVI maps for 2019 and 2024 clearly illustrate

the variation in land cover types across the watershed. (Karaburun, 2010; Chouhan and Rao, 2011) suggested negative NDVI values to represent water bodies, also shown in the Tawi watershed in which water bodies consistently showed the lowest NDVI values, ranging from -0.177 to 0.015 in 2019 and -0.39 to 0.015 in 2024 (Fig. 3, 4). Dense forest areas recorded the highest NDVI values, ranging from 0.36 to 0.765 in 2019 and from 0.36 to 0.833 in 2024 (Fig. 3, 4).

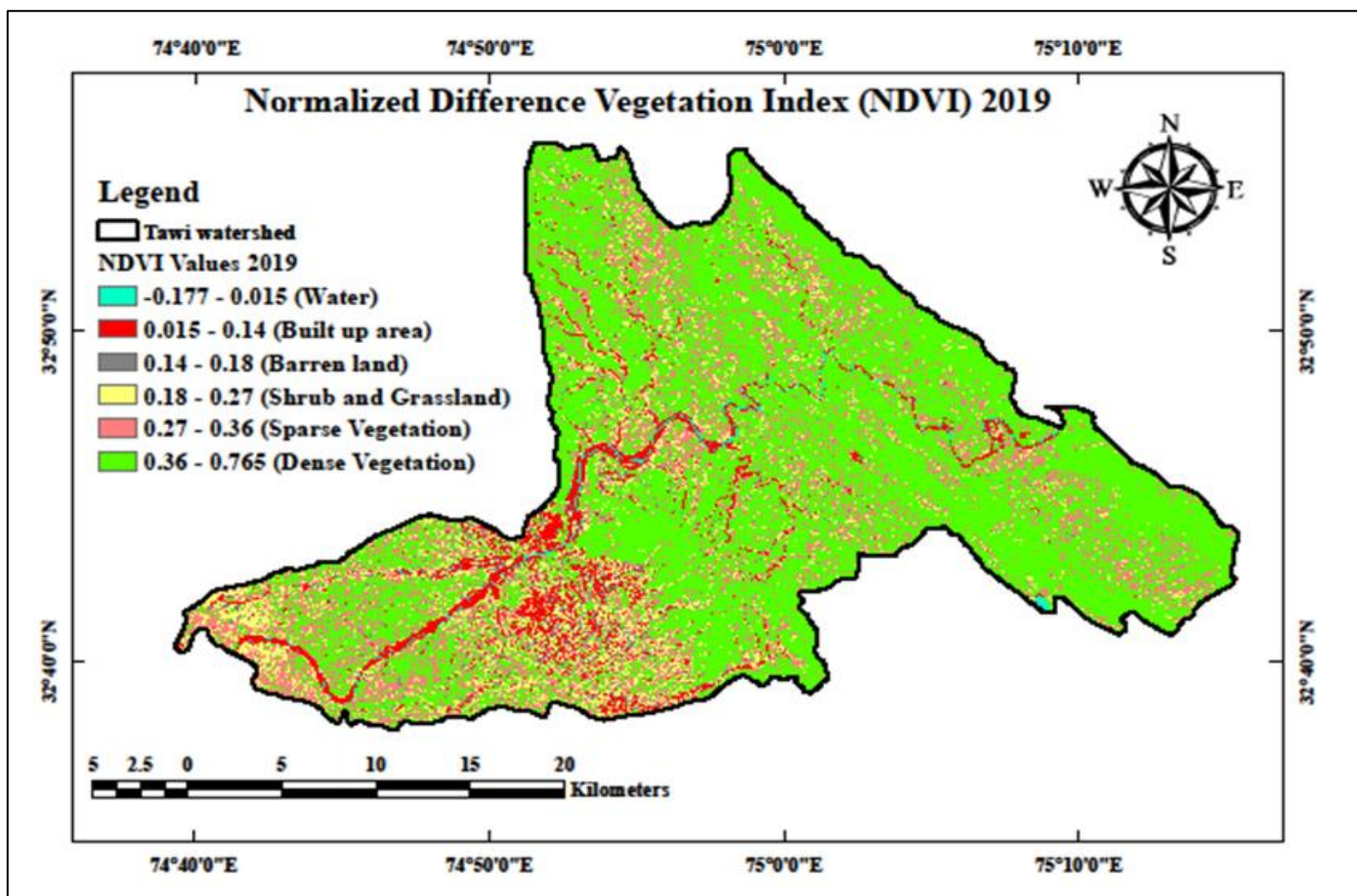


Fig 3 NDVI Map of the Tawi Watershed for 2019

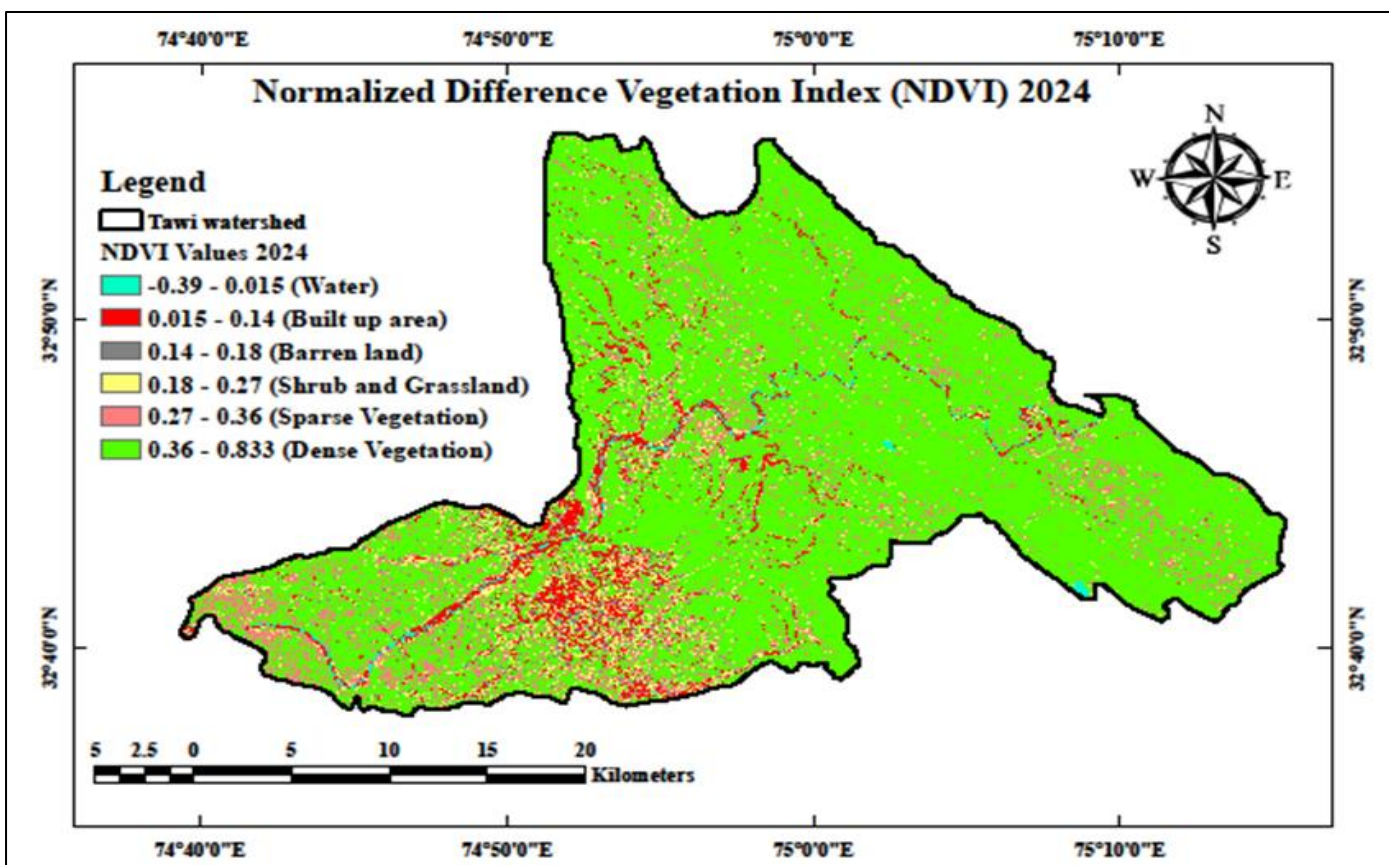


Fig 4 NDVI Map of the Tawi Watershed for 2024

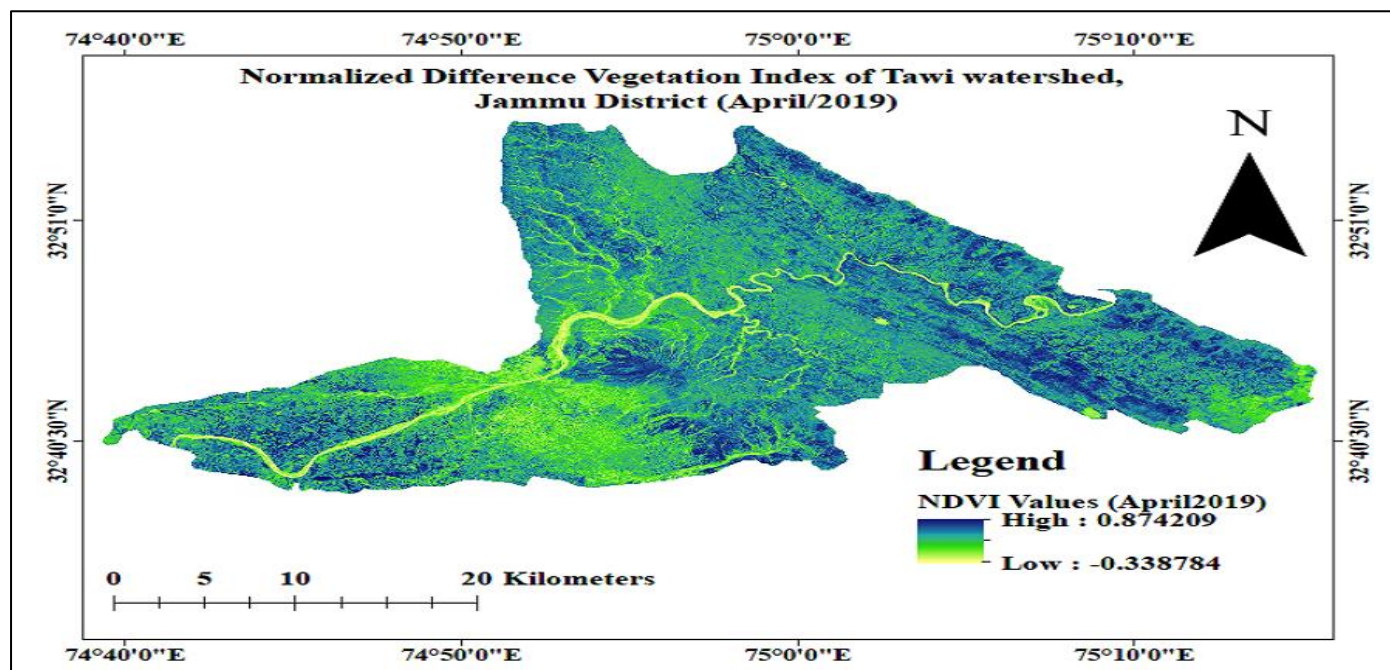


Fig 5 NDVI Map of the Tawi Watershed for April 2019

The observations indicate a significant variation in vegetation cover in the central part of the Tawi watershed, where the Tawi River flows. This area consistently shows the lowest NDVI values, as evident when comparing imagery from April and October 2019 (Figs. 5 and 6) with that from April and December 2024 (Figs. 7 and 8).

The seasonal NDVI values for the Tawi watershed demonstrate notable variation between 2019 and 2024, reflecting both temporal and spatial changes in vegetation cover. In April 2019, NDVI values ranged from a minimum of -0.34 to a maximum of 0.87, while October 2019 showed a slightly broader range, from -0.35 to 0.89. These values

suggest healthy vegetation during the post-monsoon season, with moderately high vegetation activity also observed in the pre-monsoon period.

In contrast, the NDVI values recorded in 2024 show more extreme variation. April 2024 displayed a significantly wider range, with values spanning from -1.0 to 0.95. This unusually low minimum indicates areas with exposed water bodies, barren land, while the higher maximum suggests dense vegetation in certain parts of the watershed. December 2024 NDVI values ranged from -0.52 to 0.87, indicating reduced vegetation activity during the winter season, possibly due to lower temperatures and seasonal senescence.

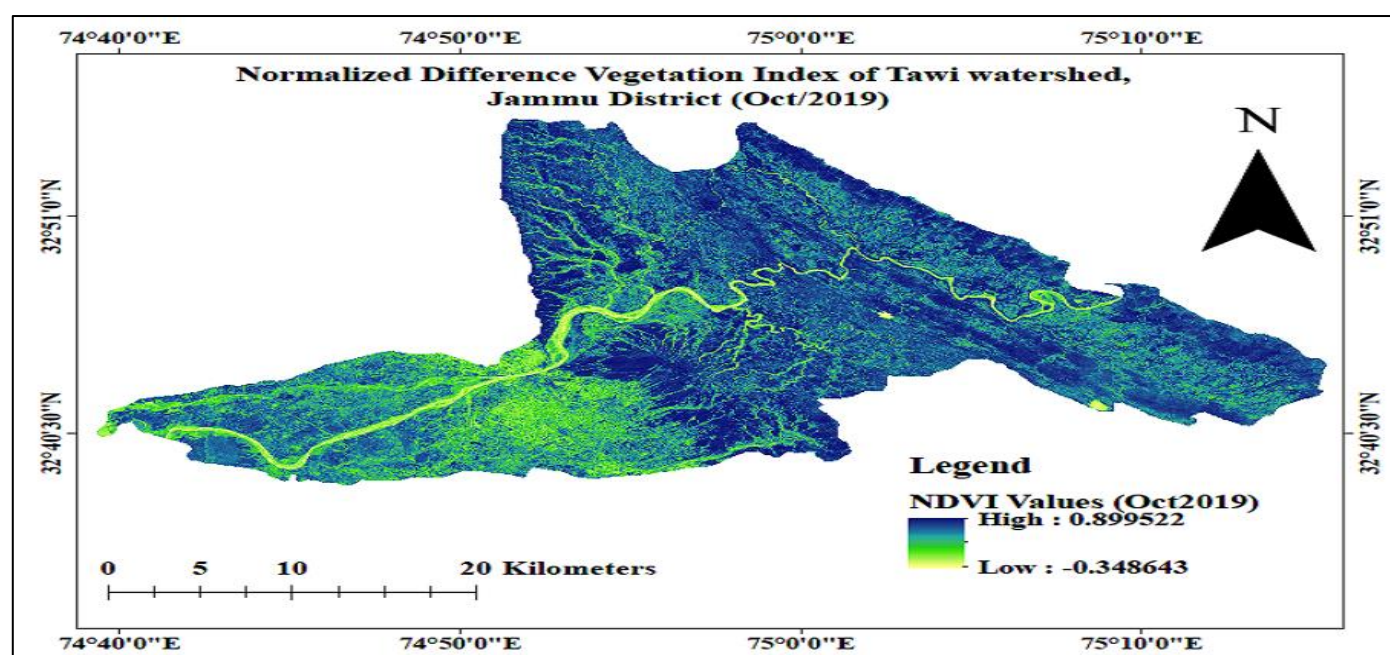


Fig 6 NDVI Map of the Tawi Watershed for October 2019

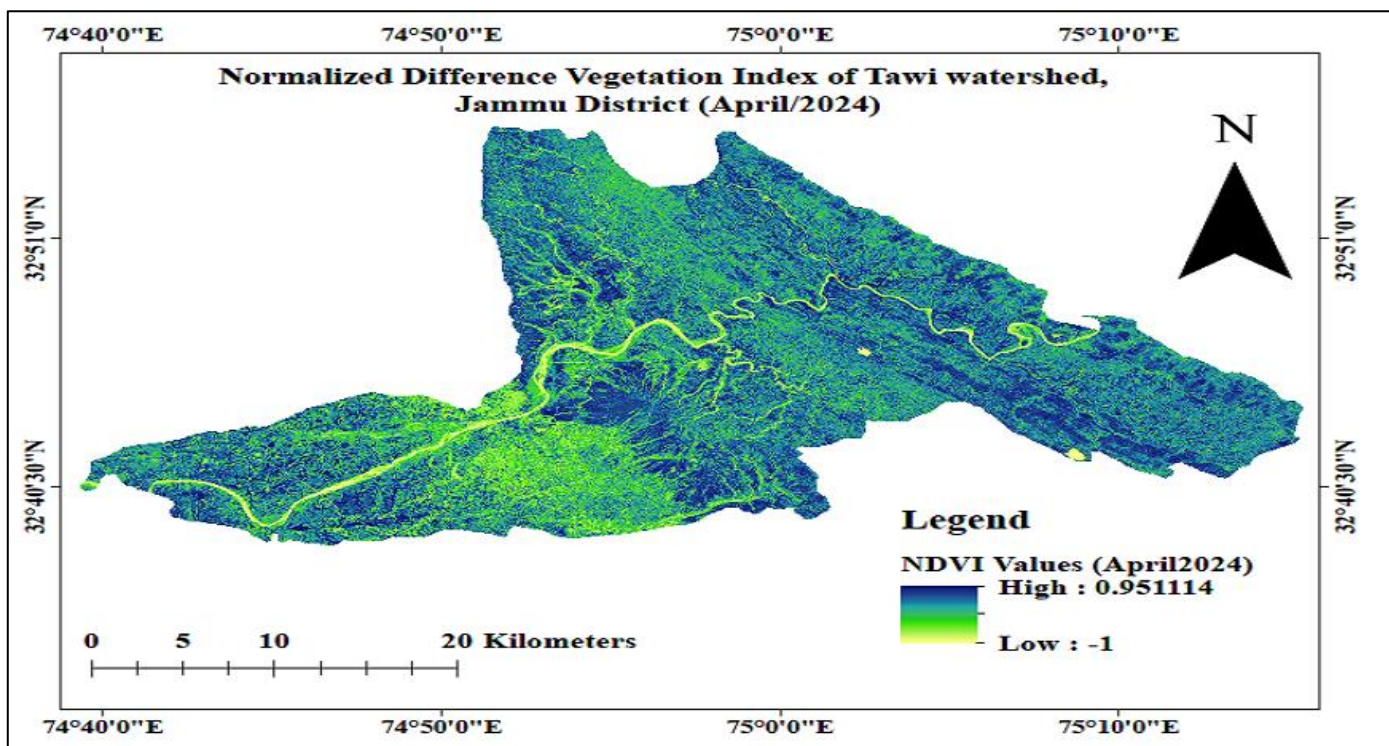


Fig 7 NDVI Map of the Tawi Watershed for April 2024

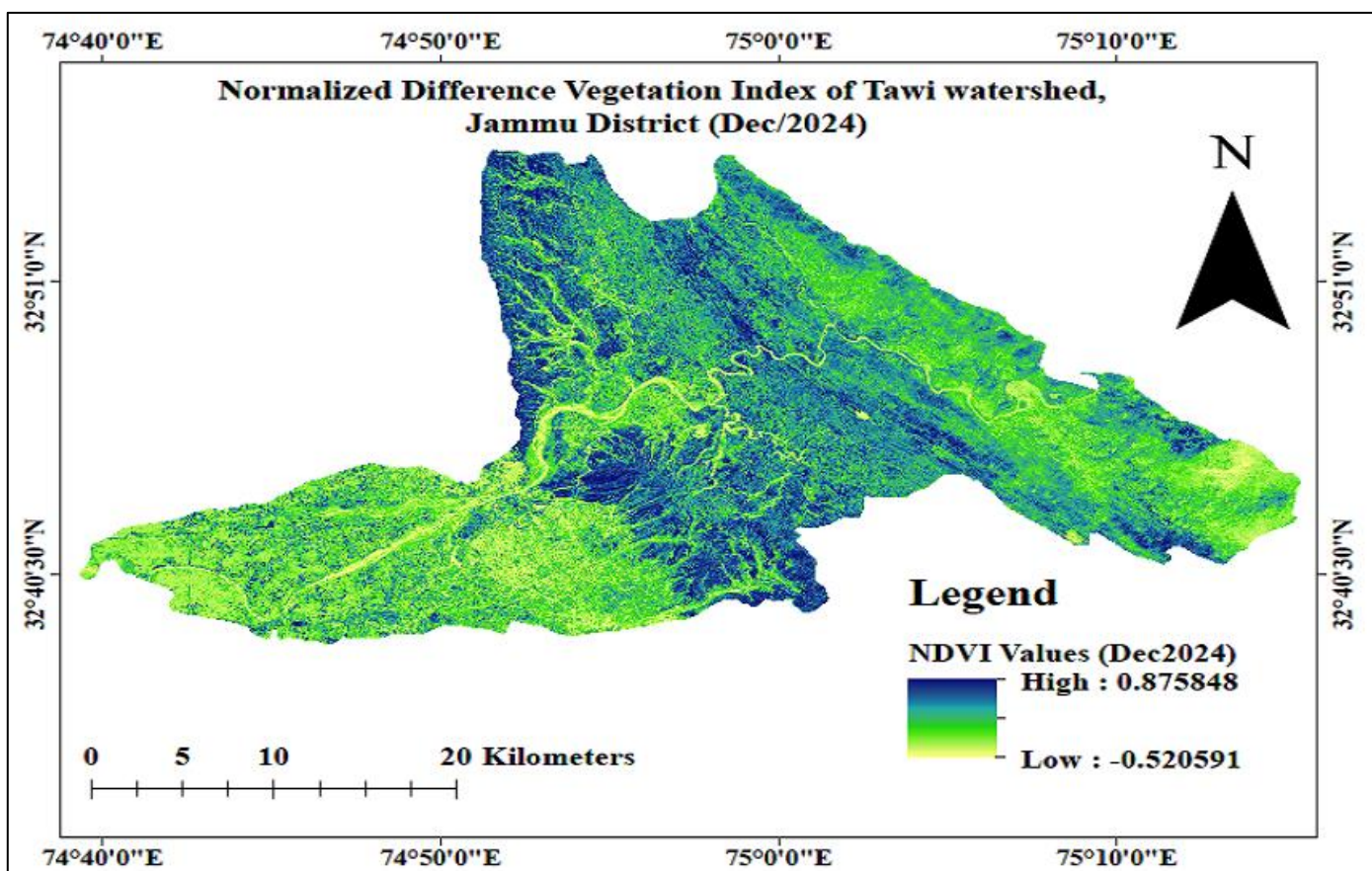


Fig 8 NDVI Map of the Tawi Watershed for December 2024

Overall, the observed changes between 2019 and 2024 point toward dynamic land cover conditions within the watershed, potentially influenced by climatic variability, land use changes, or anthropogenic impacts. The wider NDVI

range in 2024, particularly the extreme negative values, warrants further investigation to determine underlying causes such as land degradation, urban expansion, or any other reason.

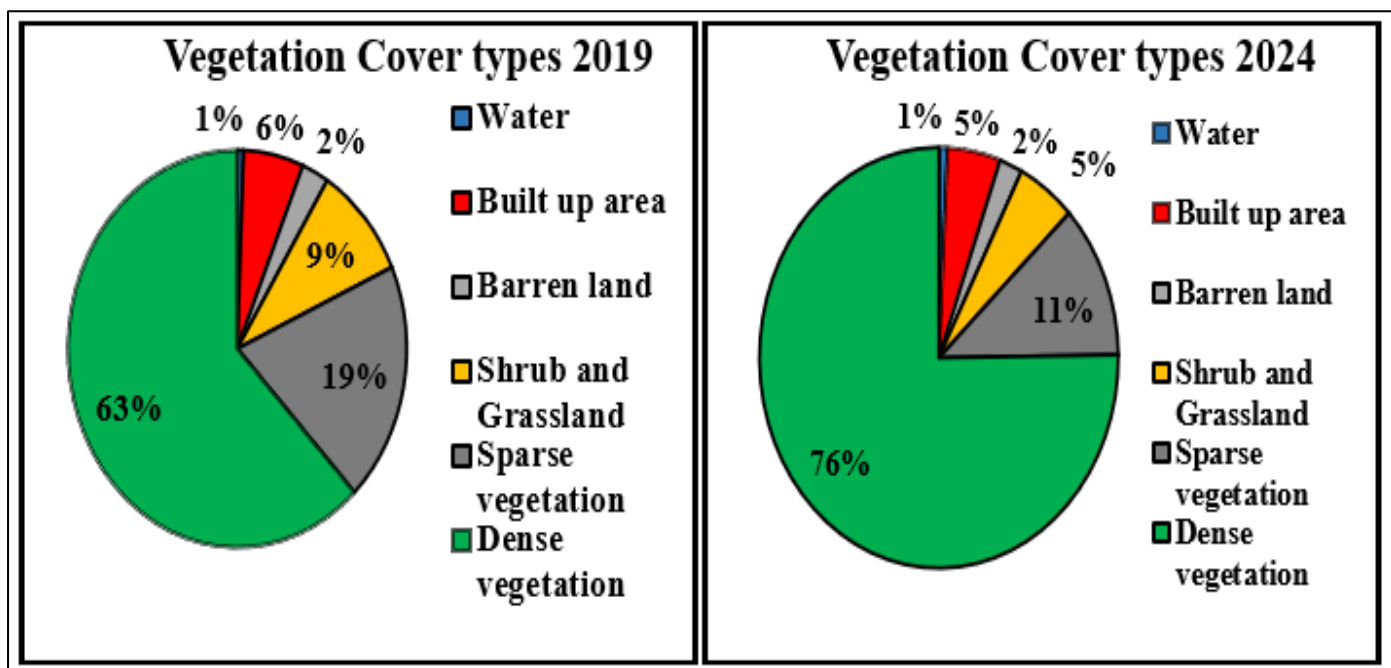


Fig 9 Pie Chart Showing Vegetation Cover Types of the Tawi Watershed for 2019 and 2024.

The areal extent of various land cover types in the Tawi watershed shows notable changes between 2019 and 2024 (Table 2). The area covered by water increased from 0.61% in 2019 to 0.77% in 2024, while dense vegetation expanded significantly from 62.14% to 75.23% (Fig. 9). In contrast, there was a decrease in built-up areas, from 5.72% in 2019 to

4.79% in 2024, and in barren land, which declined from 2.59% to 2.08% in the Tawi watershed of Jammu district (Fig. 9). Similarly, shrub and grassland cover decreased from 9.36% in 2019 to 5.30% in 2024, and sparse vegetation reduced from 19.58% to 11.84% over the same period as shown in Table 2 (Fig. 9).

Table 2 Different Vegetation Cover Types with Area (Sq Km) and Percent Area for 2019 and 2024

| Cover type | Area (Sq km) 2019 (%) | Area (Sq km) 2024 (%) |
|---------------------|-----------------------|-----------------------|
| Water | 5.02 (0.60 %) | 6.38 (0.76%) |
| Built up area | 48.20 (5.77 %) | 40.43 (4.84 %) |
| Barren land | 20.74 (2.48 %) | 16.71 (2.00 %) |
| Shrub and Grassland | 77.76 (9.32 %) | 44.04 (5.28 %) |
| Sparse vegetation | 161.29 (19.32 %) | 95.23 (11.41 %) |
| Dense vegetation | 521.71 (62.50 %) | 631.95 (75.71 %) |
| Total | 834.72 (100 %) | |

➤ *Land and Surface Temperature (LST)*

The analysis of Land Surface Temperature (LST) data for the Tawi watershed reveals significant spatial and seasonal variability between the years 2019 and 2024. These variations reflect changing climatic conditions, land cover dynamics, and possibly increased anthropogenic influence within the watershed. In April 2019, LST values ranged from a minimum of 17.8°C to a maximum of 35.2°C (Fig. 10), indicating moderate pre-monsoon heating conditions. By October 2019, the post-monsoon season brought a slight reduction in temperature, with values ranging between 16.1°C and 32.3°C (Fig. 11), likely due to increased moisture and vegetative cooling following the monsoon season.

However, the LST values in 2024 exhibit a noticeable upward shift, particularly in the pre-monsoon period. In April 2024, maximum temperatures peaked at 41.1°C while the minimum rose to 20.8°C (Fig. 12), suggesting more intense surface heating and possibly increased urban heat island

effects or land degradation. This significant rise compared to 2019 reflects potential impacts of climate variability and reduced vegetation cover, as corroborated by NDVI analysis. December 2024, representing winter conditions, showed a substantial drop in LST, with minimum and maximum values of 9.7°C and 22.5°C respectively (Fig. 13). These lower temperatures are consistent with seasonal cooling, though the slightly elevated maximums compared to typical winter norms may point to reduced surface albedo or increased built-up areas.

Overall, the temporal comparison underscores a warming trend, particularly evident in April 2024, which could be indicative of broader environmental changes such as deforestation, urbanization, or shifts in regional climate patterns. This rise in LST, especially during the warmer months, may have significant implications for local hydrology, agriculture, and ecosystem health within the Tawi watershed.

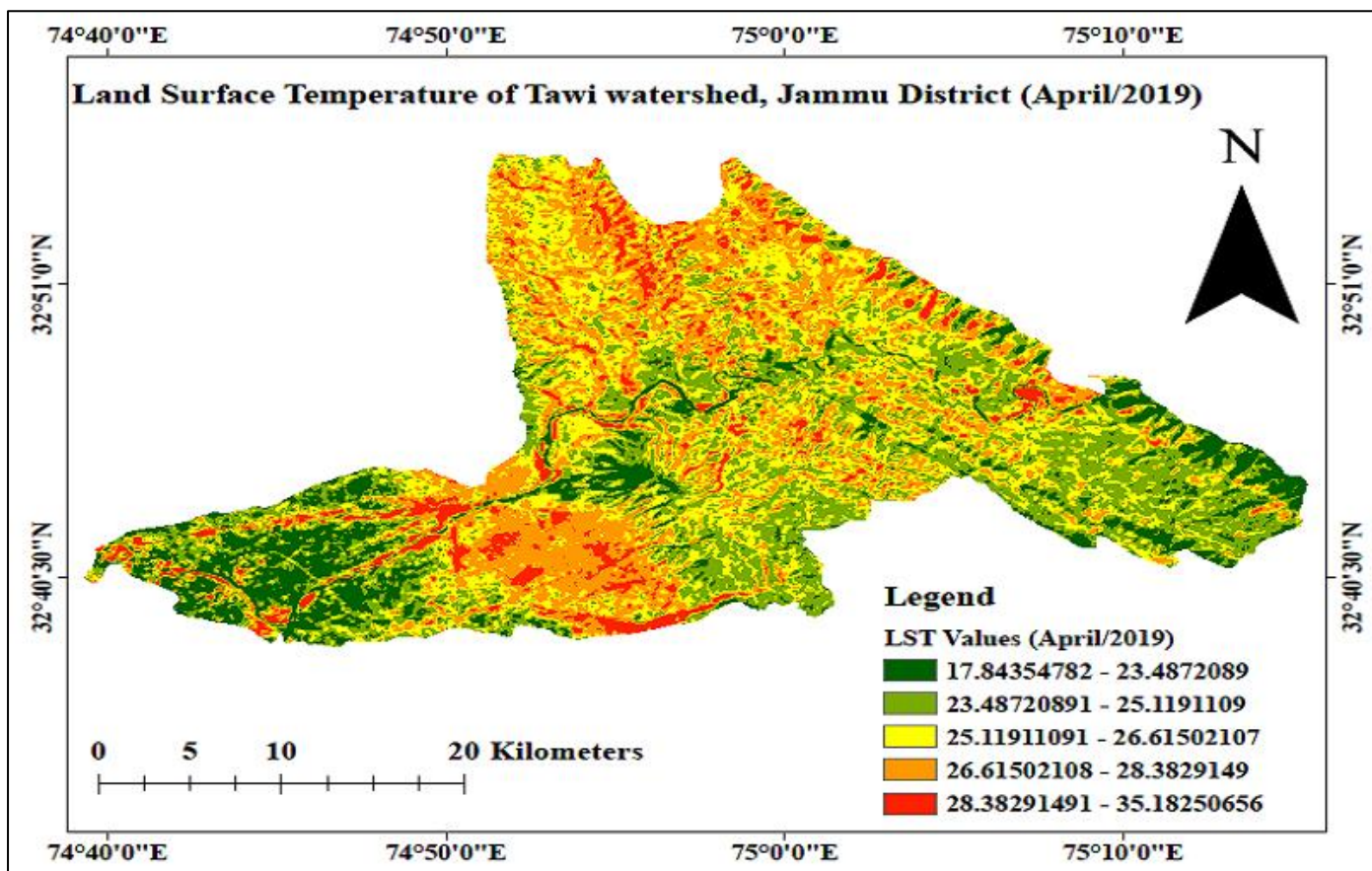


Fig 10 LST Map of the Tawi Watershed for April 2019

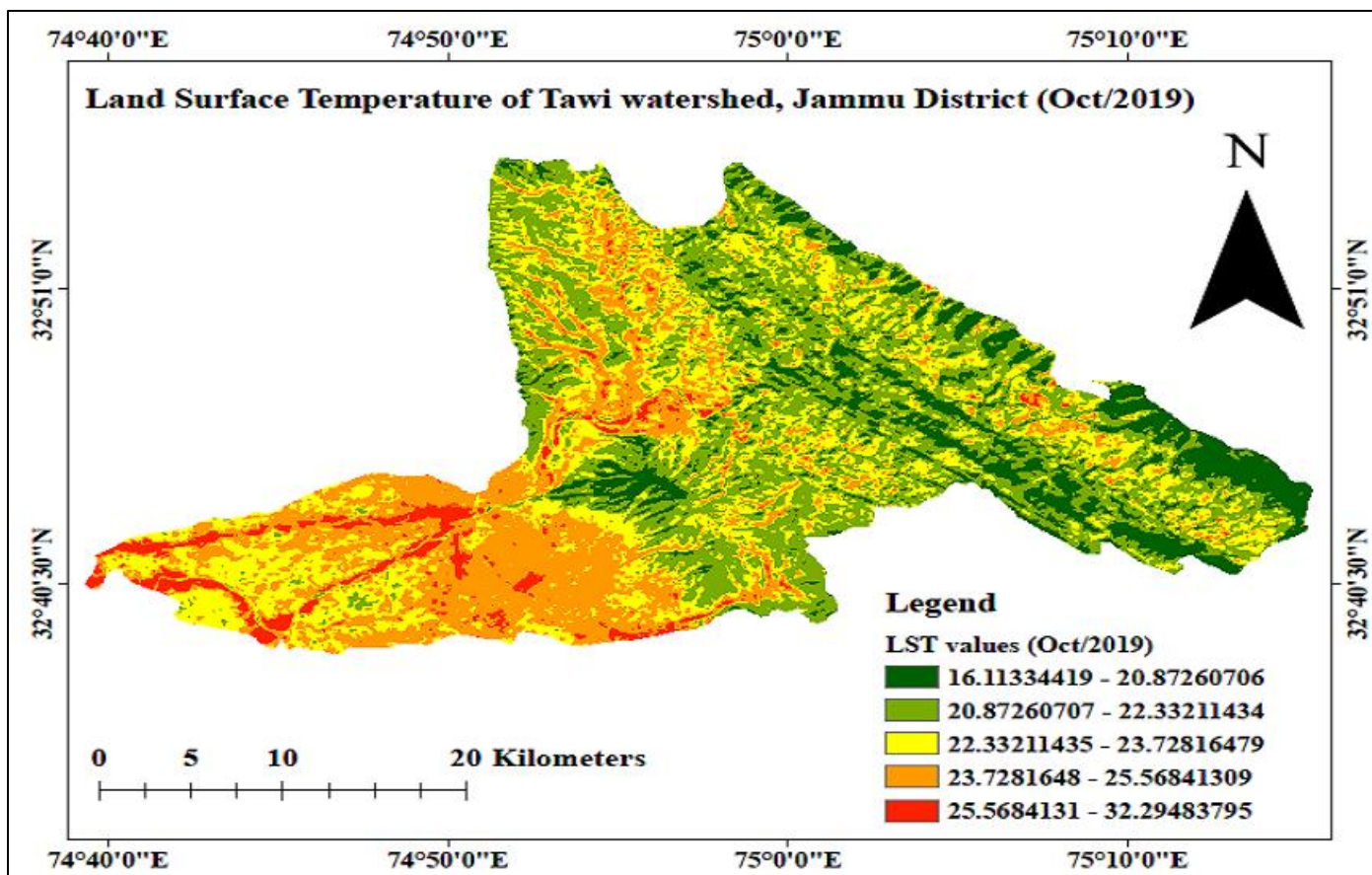


Fig 11 LST Map of the Tawi Watershed for October 2019

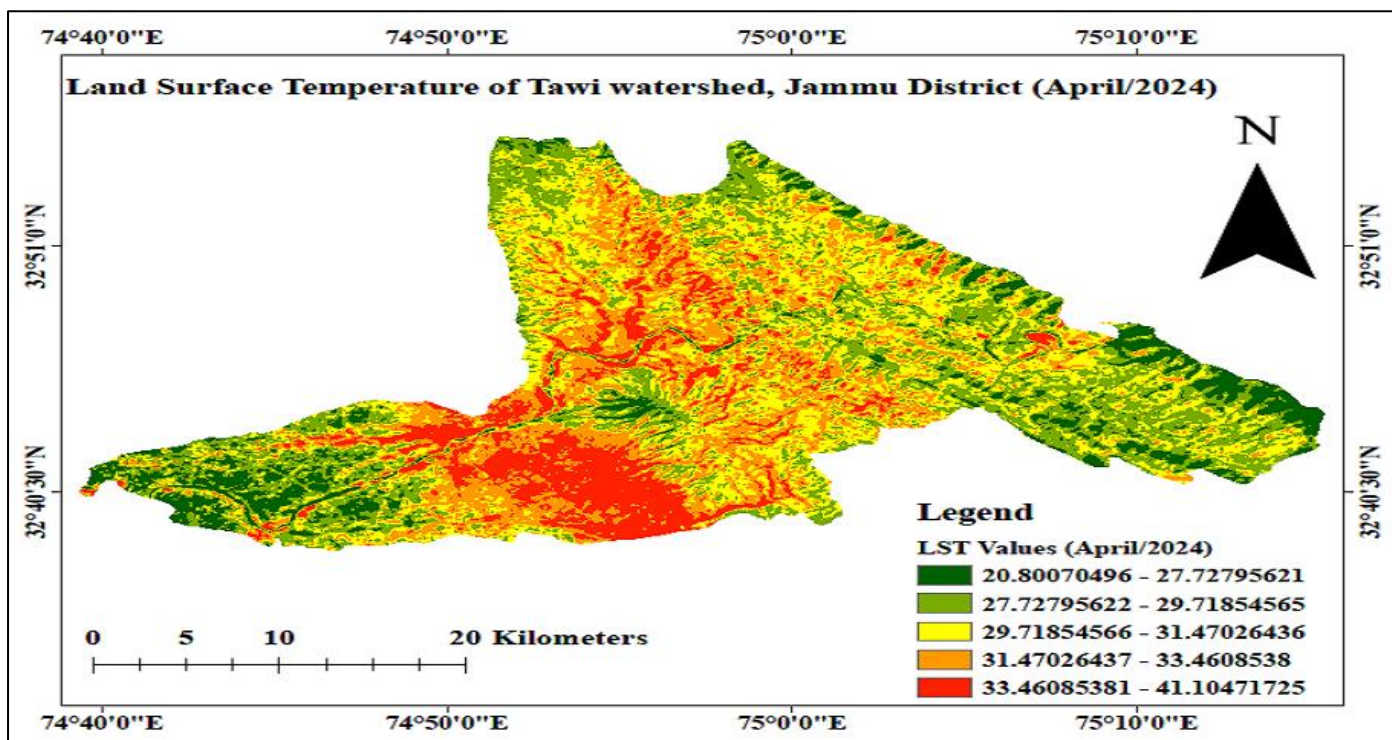


Fig 12 LST Map of the Tawi Watershed for April 2024

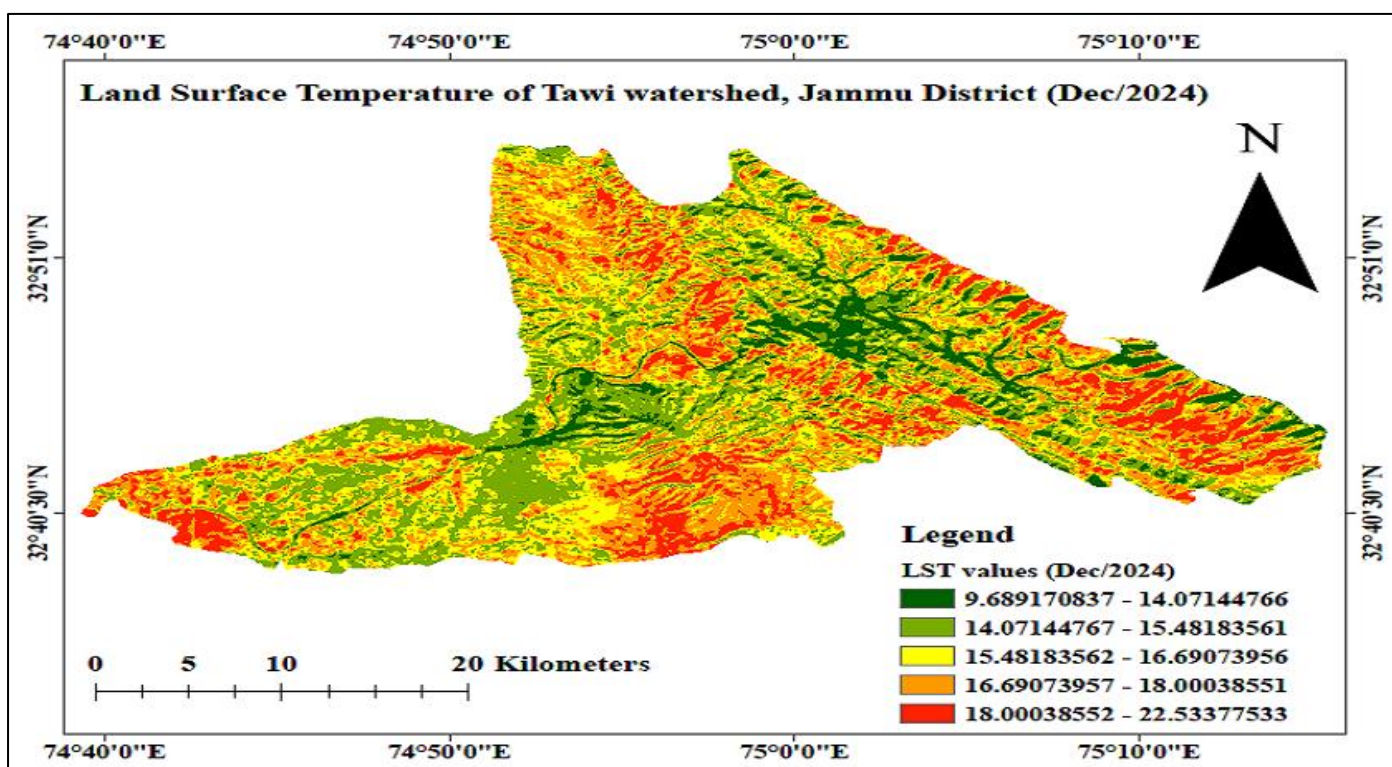


Fig 13 LST Map of the Tawi Watershed for December 2024

➤ *Correlation Between Land Surface Temperature (LST) and Normalized Difference Vegetation Index (NDVI)*

For correlation of NDVI and LST, Satellite imagery was pre-processed to derive NDVI and LST raster layers. Further, a fishnet grid was generated in ArcGIS software to create a regular pattern of sampling points across the Tawi watershed which was meant for consistent and spatially distributed data extraction. Using the "Extract Multi Values to Points" tool in

ArcGIS software, NDVI and LST values were extracted at the centroid of each fishnet cell. This tool assigned the corresponding pixel values of the NDVI and LST rasters to the points within the fishnet grid. The point feature class with the extracted NDVI and LST values was exported to a Excel worksheet which helps in the correlation between NDVI and LST values.

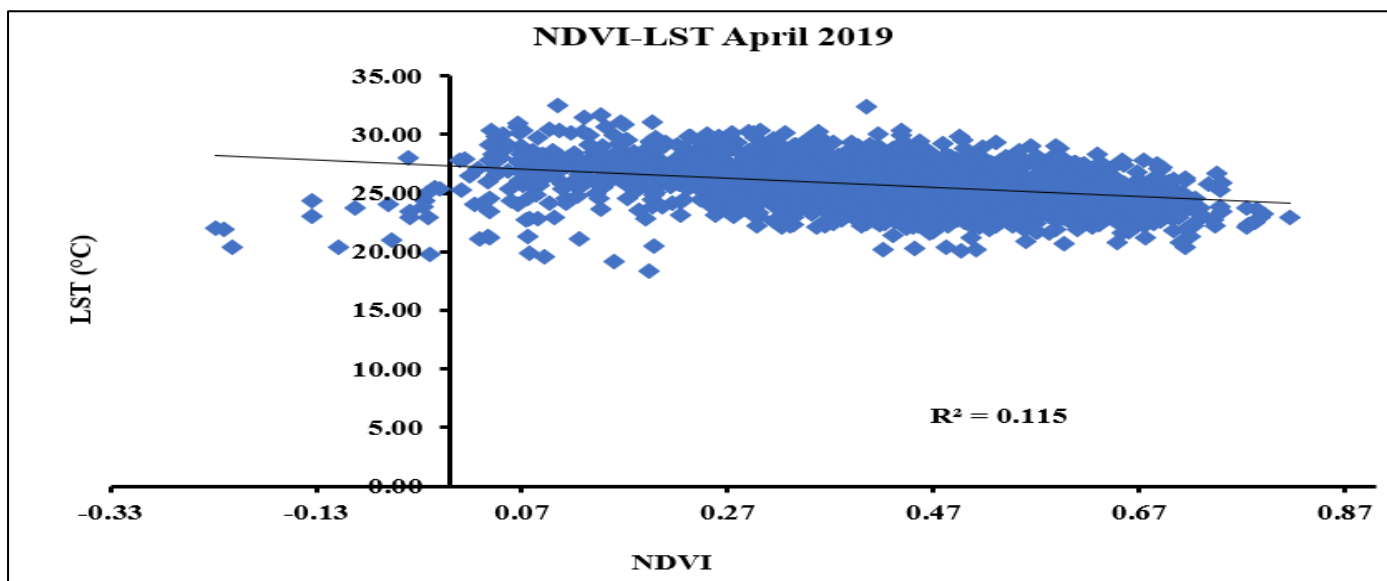


Fig 14 Correlation Between NDVI-LST During the Month of April, 2019.

The relationship between Land Surface Temperature (LST) and the Normalized Difference Vegetation Index (NDVI) is exemplified using linear regression model as:

- $LST = -3.859 NDVI + 27.30$ ($R = -0.339$; April 2019)eq 1
- $LST = -4.787 NDVI + 25.45$ ($R = -0.629$; October 2019)eq 2
- $LST = -4.909 NDVI + 33.14$ ($R = -0.447$; April 2024) eq 3
- $LST = -0.990 NDVI + 16.63$ ($R = -0.114$; December 2024) eq 4

During April 2019, the negative slope of -3.859 (eq. 1) indicates an inverse linear relationship between NDVI and LST, suggesting that areas with higher vegetation cover tend to exhibit lower land surface temperatures (Fig. 14). The coefficient of determination ($R^2 = 0.115$) indicates that only 11.5% of the variance in LST can be explained by NDVI. This reflects a weak negative linear correlation, with the corresponding Pearson correlation coefficient ($R = -0.339$). While the relationship is statistically present, it suggests that additional environmental or surface factors beyond NDVI contribute more substantially to variations in LST.

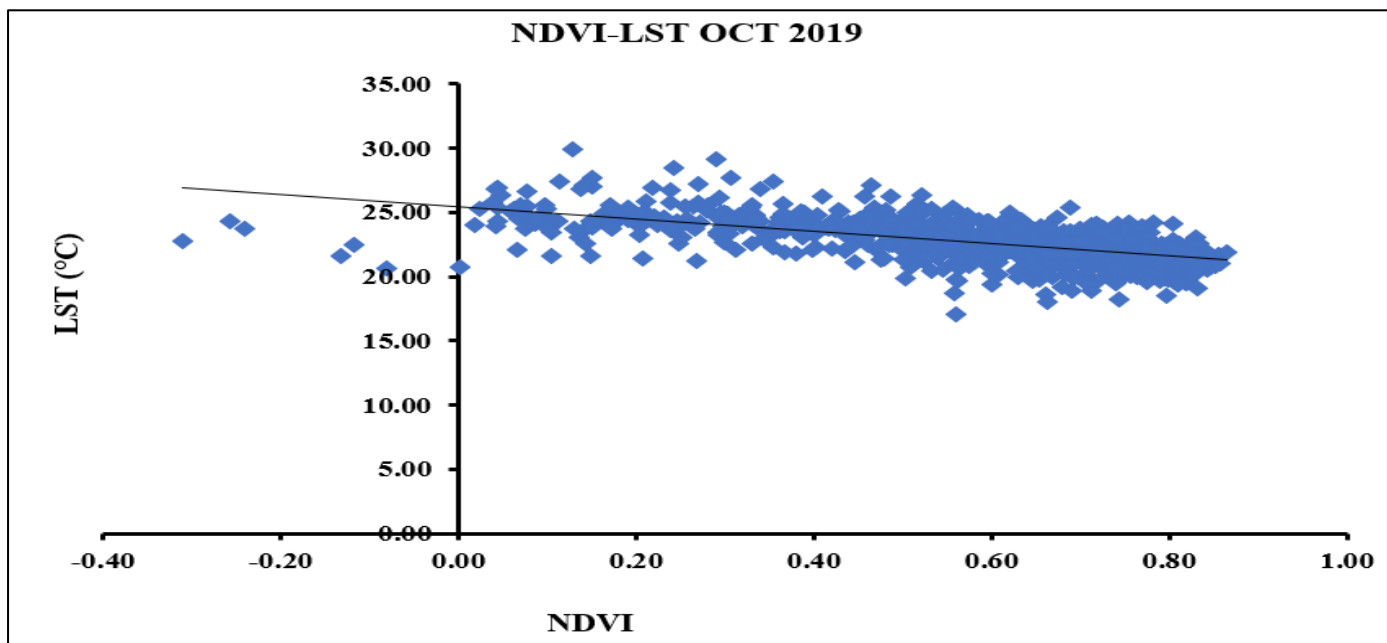


Fig 15 Correlation Between NDVI-LST During the Month of October, 2019.

During October 2019, the regression equation illustrates a negative linear relationship between the Normalized Difference Vegetation Index (NDVI) and Land Surface Temperature (LST). The negative slope of -4.787 (eq. 2)

indicates that as NDVI increases (higher vegetation density), LST tends to decrease (Fig. 15). The coefficient of determination ($R^2 = 0.396$) suggests that 39.6% of the variability in LST can be explained by variations in NDVI.

This represents a moderate negative linear correlation with Pearson correlation coefficient ($R = -0.629$).

plays a significant role in modulating surface temperature, though other environmental variables also contribute to the remaining 60.4% of the variation in LST.

This indicates a moderately strong negative correlation between NDVI and LST. In other words, vegetation cover

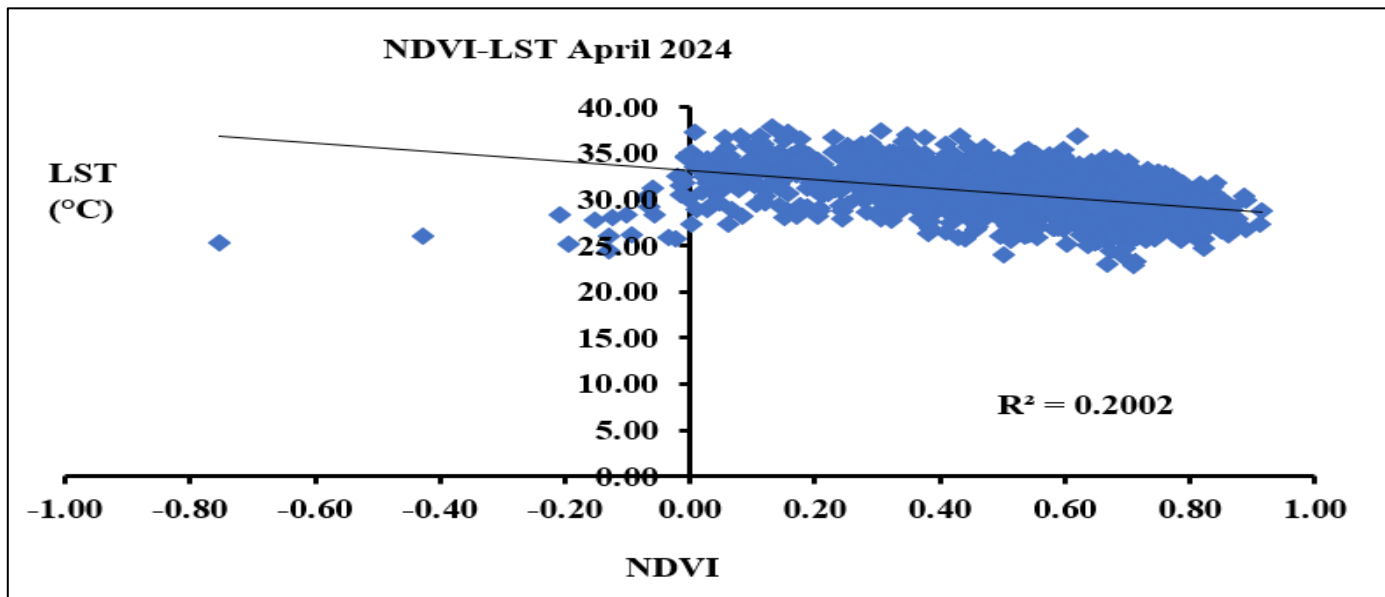


Fig 16 Correlation Between NDVI-LST During the Month of April, 2024.

During April 2024, the negative slope of -4.909 (eq. 3) suggesting that higher vegetation cover is associated with lower surface temperatures (Fig. 16). The coefficient of determination ($R^2=0.200$) implies that approximately 20% of the variability in LST is explained by changes in NDVI. This suggests a weak to moderate negative correlation with the Pearson correlation coefficient ($R = -0.447$). This indicates a moderate negative correlation between NDVI and LST. While NDVI plays a role in influencing LST, the remaining 80% of the variability is likely explained by other environmental, climatic, or land use factors.

During December 2024, the negative slope of -0.990 (eq. 4) with the coefficient of determination ($R^2 =0.013$) suggests that only 1.3% of the variability in LST is explained by NDVI (Fig. 17). This extremely low value indicates that the linear relationship between NDVI and LST is very weak and statistically insignificant with Pearson correlation coefficient ($R= -0.114$). This confirms a very weak negative correlation, implying that NDVI has little to no meaningful influence on LST in this particular case. The vast majority (98.7%) of LST variation is likely due to other environmental or anthropogenic factors not captured by NDVI alone.

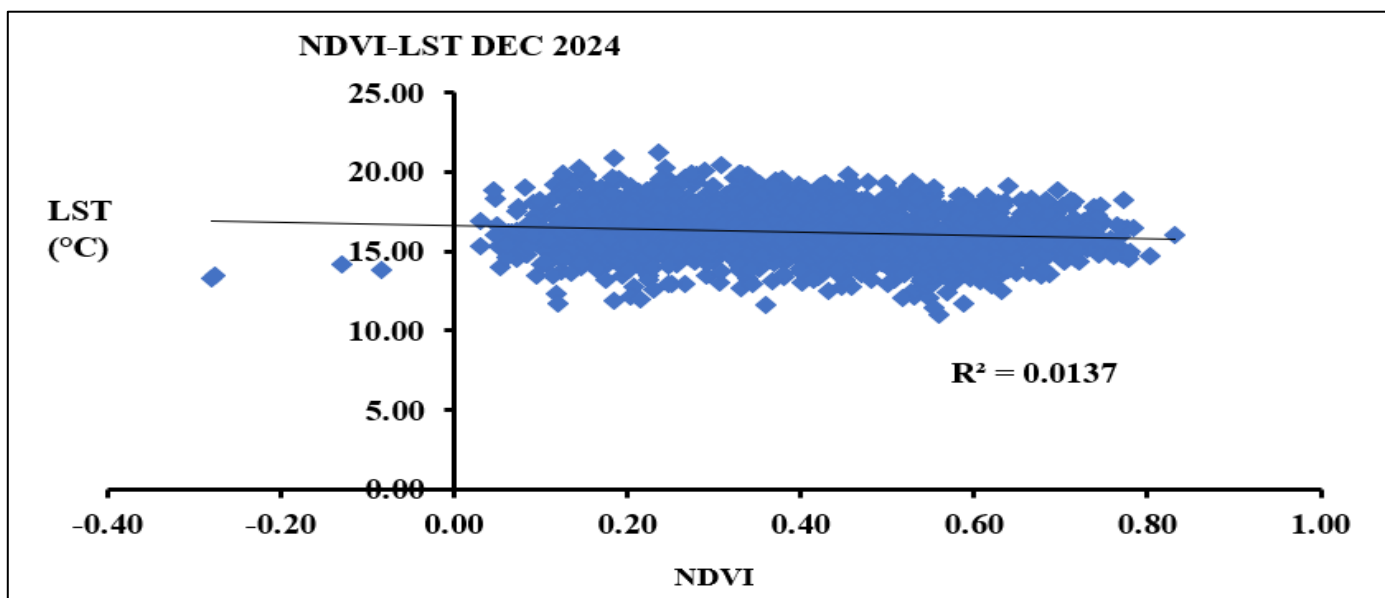


Fig 17 Correlation Between NDVI-LST During the Month of December, 2024.

➤ *Deforestation and Afforestation*

The analysis of vegetation dynamics in the Tawi watershed between 2019 and 2024 reveals significant land cover changes due to deforestation and afforestation processes (Fig. 19). The largest category, “Vegetation (Unchanged)”, covers approximately 425.93 square kilometers, indicating that a substantial portion of the watershed remained vegetated throughout the study period. Similarly, “No Vegetation (Unchanged)” accounts for about 268.79 square kilometers, representing areas that remained consistently barren or non-vegetated (Fig. 18).

Notably, afforestation areas where vegetation has newly developed covers around 39.54 square kilometers, suggesting positive vegetation growth, likely due to natural regeneration or reforestation efforts. In contrast, deforestation, representing the loss of vegetative cover, affects approximately 100.38 square kilometers (Fig. 18).

These figures indicate that the area lost to deforestation significantly exceeds the gains from afforestation, resulting in a net decline in overall vegetation cover across the watershed.

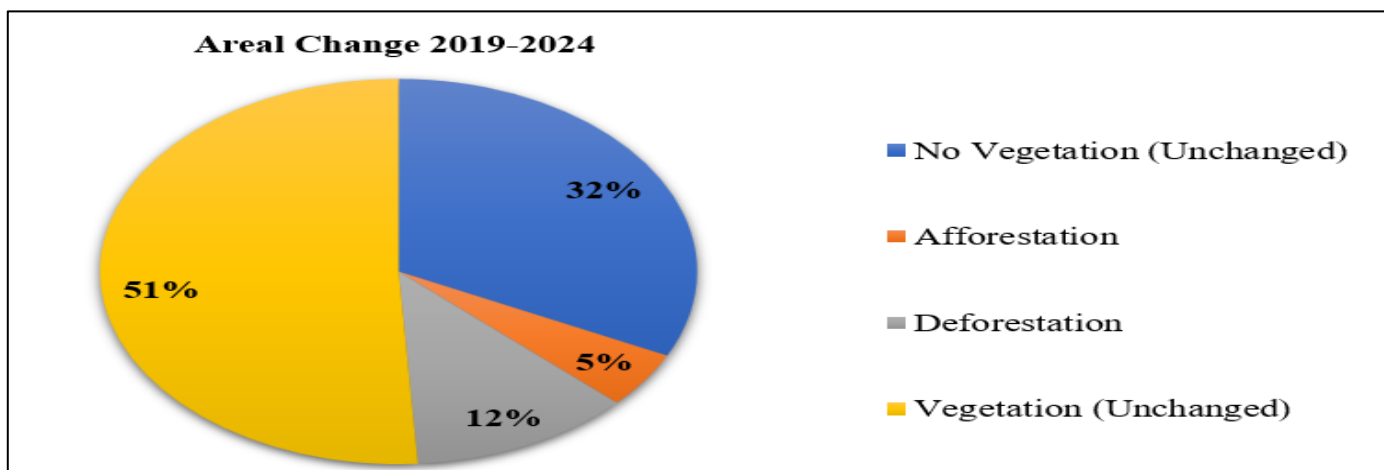


Fig 18 Afforestation and Deforestation (2019 - 2024).

Approximately 5% of the total area of the Tawi watershed experienced afforestation, indicating a positive shift from non-vegetated to vegetated land. This change may be attributed to natural regeneration, reforestation initiatives or improved land management practices. Such expansion in vegetation cover contributes to enhanced ecosystem services, carbon sequestration, and biodiversity conservation.

In contrast, about 12% of the total area underwent deforestation, reflecting a more extensive loss of vegetative

cover. This level of deforestation poses significant ecological risks, particularly in areas that are biodiversity-rich or environmentally fragile.

The proportion of land lost to deforestation (12%) is more than three times the area gained through afforestation (5%), indicating a net negative trend in vegetation cover during the study period. This imbalance highlights an ecologically unsustainable trajectory with potential long-term consequences for ecosystem stability and resilience.

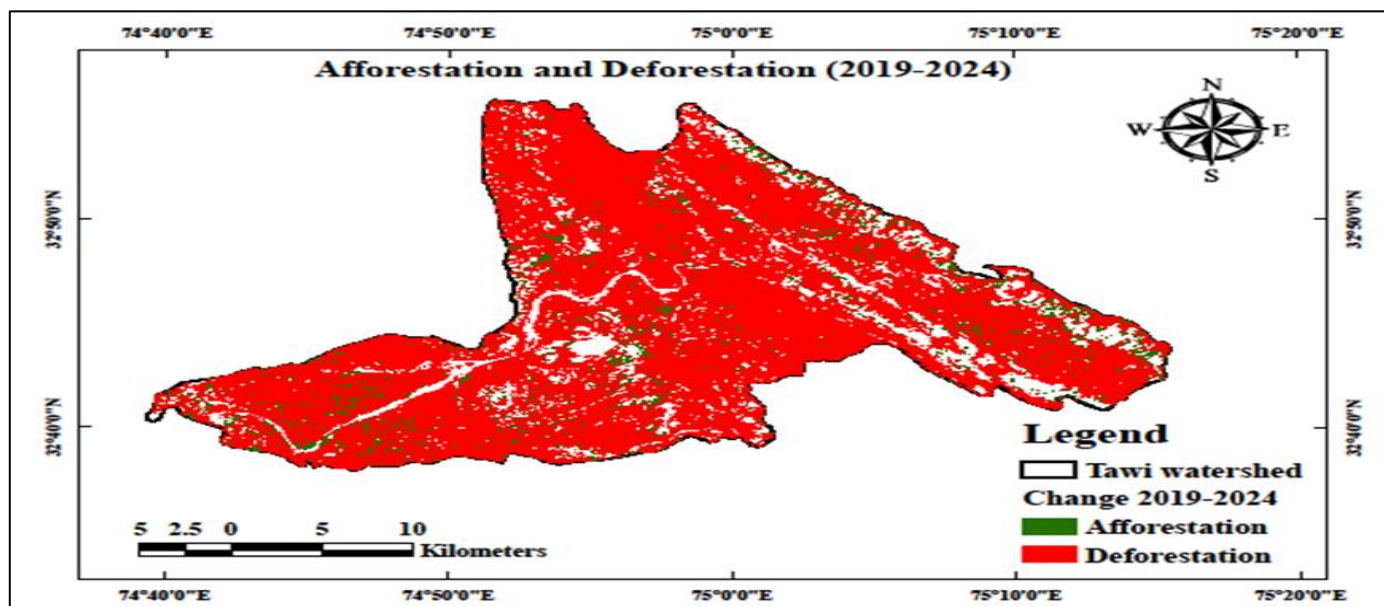


Fig 19 Afforestation and Deforestation Map of the Tawi Watershed (2019 to 2024).

➤ *Tree Cover Trends in Relation to Afforestation and Deforestation*

As per seasonal pattern, the tree cover is consistently lowest during June and July across all years (Fig. 20). A sharp increase is observed in August and September, suggesting this period may coincide with peak growing season or monsoon rains, encouraging vegetation growth and also likely timing for afforestation activities or natural regeneration. During afforestation years in 2023-24, the tree cover in March, August, and September reaches the highest

values across the 6-year period. This corresponds well with the 5% afforestation confirming a net increase in vegetation cover in recent years. These peaks suggest that afforestation efforts have been both effective and sustained, especially around the mid-year (possibly post-monsoon). Similarly, deforestation may also be reflected in June/July, which appears to rise even more sharply in some years (e.g., 2024, 2021). The overall trend shows that the Tree cover has generally increased from 2020 to 2024, with 2024 showing the highest overall coverage in several months.

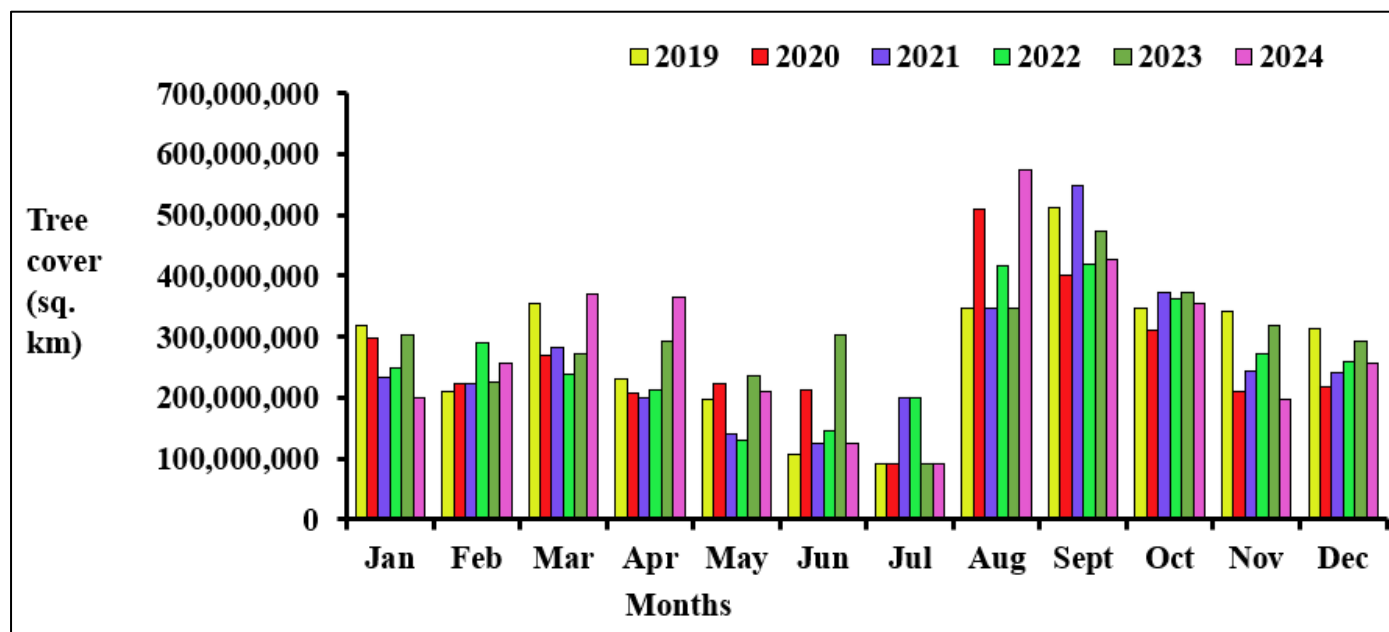


Fig 20 Graph Showing Month Wise Tree Cover in Tawi Watershed from 2019 to 2024

V. DISCUSSION

The integrated analysis of NDVI and LST data from 2019 to 2024 reveals significant environmental changes across the Tawi watershed, driven by both natural and anthropogenic factors. The observed trends demonstrate a clear interrelationship between NDVI and LST, with variations in one often influencing the other.

Between 2019 and 2024, NDVI values show a wider and more extreme range, particularly in April 2024, where values span from -1.00 to 0.95. This indicates increasing spatial heterogeneity in vegetation cover, with both densely vegetated areas and barren or degraded land existence. The negative NDVI values, especially in 2024, may reflect expanding built-up areas, exposed soil, or stressed vegetation due to changing land use or climatic conditions.

Simultaneously, LST values exhibit a noticeable rise, particularly during the pre-monsoon season. April 2024 recorded a maximum LST of 41.1°C—substantially higher than the 35.2°C observed in April 2019. This increase in surface temperature is likely associated with reduced vegetation cover, as lower NDVI typically corresponds with diminished evapotranspiration and increased surface heating. The winter season also showed elevated minimum LSTs in

2024, suggesting reduced cooling capacity of the landscape, possibly due to loss of vegetative insulation.

VI. CONCLUSION

The present study suggests a strong inverse relationship between NDVI and LST values in the Tawi watershed. The areas with lower vegetation cover (low NDVI) correspond to higher surface temperatures (high LST), particularly evident in April 2024. This trend reflects potential land cover changes such as vegetation loss, urban expansion, or soil exposure, contributing to higher heat absorption and reduced evapotranspiration.

Overall, the integrated findings highlight a concerning trend: declining vegetation health and increasing land surface temperatures are mutually reinforcing processes that can accelerate environmental degradation. These dynamics point to ongoing land cover changes, potentially due to urbanization, deforestation, or climate variability. Effective watershed management strategies such as afforestation, sustainable land use planning, and urban green infrastructure are essential to mitigate these impacts and ensure long-term ecological resilience in the Tawi watershed

The Tawi watershed has undergone a net loss in vegetation cover with deforestation (12%) significantly

outpacing afforestation (5%) over the study period. This imbalance suggests a negative environmental impact, though a comprehensive evaluation of the ecological quality of both afforested and deforested areas is essential to determine the long-term sustainability and resilience of the landscape.

Tree cover data from 2019 to 2024 reveals distinct seasonal and interannual patterns, with peaks typically occurring in August–September, likely corresponding to periods of natural vegetation growth or active afforestation. A sharp increase in 2024, particularly in March and August–September, aligns with the observed 5% afforestation trend indicating a localized net gain in vegetation during that year.

Despite some fluctuations most notably minor dips likely associated with ongoing deforestation (12%), the overall trend in tree cover is positive, suggesting that afforestation efforts have begun to yield measurable improvements in canopy cover. However, this gain does not yet offset the broader loss, underscoring the need for sustained and ecologically sound restoration strategies.

REFERENCES

- [1]. Molnár, T., & Király, G. (2023). Forest monitoring based on Sentinel-2 satellite imagery, Google Earth Engine cloud computing, and machine learning. *Preprints. doi, 10*.
- [2]. Tucker, C. J. (1979). Red and photographic infrared linear combinations for monitoring vegetation. *Remote sensing of Environment, 8*(2), 127-150.
- [3]. Ihlen, V., & Zanter, K. (2019). Landsat 8 (L8) data users handbook. *US Geological Survey, 670*.
- [4]. Karaburun, A. (2010). Estimation of C factor for soil erosion modeling using NDVI in Buyukcekmece watershed. *Ozean Journal of applied sciences, 3*(1), 77-85.
- [5]. Chouhan, R., & Rao, N. (2011). Vegetation detection in multispectral remote sensing images: Protective role-analysis of vegetation in 2004 indian ocean tsunami. *PDPM Indian Institute of Information Technology*.
- [6]. Scanlon, T. M., Albertson, J. D., Caylor, K. K., & Williams, C. A. (2002). Determining land surface fractional cover from NDVI and rainfall time series for a savanna ecosystem. *Remote Sensing of Environment, 82*(2-3), 376-388.
- [7]. Kunkel, M. L., Flores, A. N., Smith, T. J., McNamara, J. P., & Benner, S. G. (2011). A simplified approach for estimating soil carbon and nitrogen stocks in semi-arid complex terrain. *Geoderma, 165*(1), 1-11.
- [8]. Anbazhagan, S., & Paramasivam, C. R. (2016). Statistical correlation between land surface temperature (LST) and vegetation index (NDVI) using multi-temporal landsat TM data. *International Journal of Advanced Earth Science and Engineering, 5*(1), 333-346.
- [9]. Smith, R. C. G., & Choudhury, B. J. (1990). On the correlation of indices of vegetation and surface temperature over south-eastern Australia. *International Journal of Remote Sensing, 11*(11), 2113-2120.
- [10]. Julien, Y., Sobrino, J. A., & Verhoef, W. (2006). Changes in land surface temperatures and NDVI values over Europe between 1982 and 1999. *Remote sensing of environment, 103*(1), 43-55.
- [11]. Yuan, X., Wang, W., Cui, J., Meng, F., Kurban, A., & De Maeyer, P. (2017). Vegetation changes and land surface feedbacks drive shifts in local temperatures over Central Asia. *Scientific Reports, 7*(1), 3287.
- [12]. Leprieux, C., Kerr, Y. H., Mastorchio, S., & Meunier, J. C. (2000). Monitoring vegetation cover across semi-arid regions: comparison of remote observations from various scales. *International Journal of Remote Sensing, 21*(2), 281-300.
- [13]. Liu, H. Q., & Huete, A. (1994, August). A system-based modification of the NDVI to minimize soil and atmospheric noise. In *Proceedings of IGARSS'94-1994 IEEE International Geoscience and Remote Sensing Symposium* (Vol. 1, pp. 128-130). IEEE.
- [14]. Karunakaran, K and Ranga Rao, 1976. Status of Exploration for hydrocarbons in the Himalayan Region- Contribution ti the stratigraphy and structure-Himalayan Geology Seminar, New Delhi.
- [15]. CGWB (2013). Groundwater Information Booklet of Jammu District. Ministry of Water Resources, Government of India.